J. Fluid Mech. (1982), *vol.* 120, *pp.* 433–450
Printed in Great Britain

On flow between counter-rotating cylinders

By C. A. JONES
School of Mathematics, University of Newcastle upon Tyne, U.K.

(Received 5 March 1981 and in revised form 3 December 1981)

Axisymmetric flows between counter-rotating cylinders of varying radius ratio are examined. The stability of these flows to non-axisymmetric disturbances is considered, and the results of these calculations are compared with experiments.

1. Introduction

The problem of incompressible flow between counter-rotating cylinders has not received quite as much attention as the case in which the outer cylinder is fixed. Nevertheless, there is a considerable body of experimental results available (e.g. Donnelly & Fultz 1960; Nissan, Nardacci & Ho 1963; Coles 1965; Snyder 1968, 1969*a*, *b*). It was therefore decided to use the methods developed in a previous paper (Jones 1981, henceforth referred to as paper I) to attack the counter-rotating cylinder problem. The main object was to see whether the areas of agreement between theory and experiment found for the fixed outer cylinder case in paper I extended to the case where $\mu = \Omega_{\text{outer}}/\Omega_{\text{inner}}$ is not equal to zero.

The basic idea is to compute axisymmetric solutions corresponding to Taylor-vortex flows, and then to consider the linear stability of these flows to non-axisymmetric perturbations. This approach is only applicable to those regions of the (η, μ)-plane ($\eta = R_{\text{inner}}/R_{\text{outer}}$) where steady axisymmetric Taylor-vortex solutions can be found. As reported by Krueger, Gross & DiPrima (1966), when η is near 1 and μ is sufficiently negative the first transition from purely azimuthal flow, called Couette flow, is a non-axisymmetric one. This theoretical result was confirmed experimentally by Snyder (1968), who observed that in these cases the subsequent flow pattern was usually one of spiral vortices rather than axisymmetric ones. In consequence our attention is restricted to values of μ in the approximate range $-0{\cdot}8 < \mu < 0$.

Donnelly & Fultz (1960) made an extensive experimental survey of the transition to Taylor vortices in the case $\eta = 0{\cdot}5$, reasonable agreement being obtained with the theoretical predictions of the critical Taylor number Ta_{v} made by Chandrasekhar (1958). The case $\eta = 0{\cdot}5$ was further explored experimentally by Snyder (1969*a*, *b*), who gave the Taylor number Ta_{w} for the transition to wavy vortices, and many details about observed axial wavelengths and the frequencies of wavy modes. Snyder (1968) has also determined experimentally points on the curve in the (η, μ)-plane dividing that plane into regions where axisymmetric vortices are found and regions where they are not; this question was also considered by Nissan *et al.* (1963).

On the theoretical side, Krueger *et al.* (1966) have given a fairly comprehensive survey of the linear theory of the first transition in the narrow gap limit. DiPrima & Grannick (1971) considered finite-amplitude effects, using the amplitude-expansion method of Davey, DiPrima & Stuart (1968), and they discovered the subcritical

instability of the Taylor-vortex mode. This is pursued further here. They also investigated the stability of the spiral mode; this is outside the scope of this paper. Nakaya (1975) has investigated the onset of waviness in the narrow-gap limit using the amplitude-expansion method.

In this paper there are three main areas of investigation. Firstly, the behaviour in the neighbourhood of the transition from azimuthal flow is considered; the region of the (η,μ)-plane given by $0{\cdot}5 < \eta < 1$ and $-0{\cdot}8 < \mu < 0$ is examined, thus extending the work of Krueger *et al.* away from the narrow-gap limit. Also, the question of subcriticality of the Taylor vortex mode is examined. The second topic considered is the behaviour of the nonlinear axisymmetric Taylor vortex solutions. The most surprising results here concern the existence and uniqueness of the nonlinear solutions. Finally, the onset of waviness from the Taylor-vortex solution is discussed; here we have had to restrict attention to selected areas of the (η,μ)-plane; a more comprehensive survey, although desirable, would have been too expensive computationally. The case $\eta = 0{\cdot}5$ has received considerable experimental attention, so this is studied here; the rest of the time was spent on fairly narrow gaps.

The cylinders are assumed to have infinite length; this means, of course, that comparison with experiment must necessarily mean large-aspect-ratio experiments. Furthermore, when wavy disturbances occur, they are assumed to be of the same axial wavenumber (or small integer multiples of the wavenumber) as that of the Taylor-vortex flow.

2. Formulation of the problem

The method of approach is similar to that in the fixed outer cylinder case discussed in paper I. However, in this problem the azimuthal flow before the onset of Taylor vortices is

$$u_\phi^0(r) = \frac{\Omega_1 R_1^2}{1-\eta^2}\left[\frac{1-\mu}{r} - \frac{(\eta^2-\mu)r}{R_1^2}\right], \tag{2.1}$$

where $\mu = \Omega_2/\Omega_1$, Ω_1 = angular velocity of inner cylinder, Ω_2 = angular velocity of outer cylinder, R_1 = radius of inner cylinder, and $\eta = R_1/R_2$ is the radius ratio. The case we are interested in has $\mu < 0$, so there is a nodal value of r at which u_ϕ^0 is zero. For values of r greater than this critical value Rayleigh's stability criterion is satisfied, so these regions do not contribute to driving the centrifugal instability.

The Taylor number is defined as

$$Ta = \frac{2\Omega_1^2 d^4(\eta^2-\mu)}{(1-\eta^2)\nu^2}; \tag{2.2}$$

there is no single obvious choice for the definition of Ta, and different authors have used different definitions. The Taylor number used by DiPrima & Grannick has a factor 4 where we have a factor 2, but is otherwise the same; the disadvantage of their definition is that in the case $\mu = 0$ most authors have $Ta = 2\Omega_1^2 d^4\eta^2/(1-\eta^2)\nu^2$, whereas their formula gives twice this value. Since we wish to compare cases where μ can be either zero or non-zero, we adopt (2.2) as the appropriate definition. We nondimensionalize using gap width $R_2 - R_1 = d$, so that $r = R_1 + xd$, $z = \zeta d$, and the viscous time scale is d^2/ν.

For the axisymmetric nonlinear problem we introduce $v = u_\phi - u_\phi^0$ and a Stokes stream function ψ; these are then expanded as

$$\psi = \sum_{n=1}^{N} \sum_{m=0}^{M} \psi_{mn} T_m^*(x) \sin n\alpha\zeta, \tag{2.3}$$

$$v = \sum_{n=0}^{N} \sum_{m=0}^{M} v_{mn} T_m^*(x) \cos n\alpha\zeta, \tag{2.4}$$

the $T_m^*(x)$ being reduced Chebyshev polynomials. When these truncated expressions are introduced into the Navier–Stokes equations, collocation at selected points gives a set of nonlinear algebraic equations for the ψ_{mn} and v_{mn}. Details of the equations and the numerical procedure are given in paper I.

The perturbations to the axisymmetric solutions are proportional to

$$\exp(\sigma t + i(\omega t - m\phi)),$$

where σ and ω are real and m is an integer. The perturbed radial and axial velocities u_r' and u_z' are chosen as dependent variables, except in the case of axisymmetric perturbations, when ψ' and v', the perturbed stream function and azimuthal velocity, are used. As in the $\mu = 0$ case disturbances can be separated into two classes: those that have perturbed axial velocity u_z' proportional to a sum of terms involving $\sin n\alpha\zeta$, which we call in-phase modes, since they are in-phase with the Taylor vortex flow; and those that have u_z' proportional to a sum of terms involving $\cos n\alpha\zeta$, the out-of-phase modes. Both possibilities have to be considered, but out-of-phase modes are usually more important.

The parameters required to determine a nonlinear axisymmetric state are Ta, η, μ and α, the axial wavenumber ($\alpha = 2\pi d/\lambda$ where λ is the wavelength). The method of solution of the nonlinear equations involves Newton–Raphson iteration from an initial guess. In many situations the nonlinear solutions are not unique, so that the solution that emerges on a particular run with a particular set of input parameters is not necessarily the only solution with those input parameters; a different solution may result if the initial guess is chosen differently. We shall discuss the question of uniqueness further in § 4. The stability calculation for a given nonlinear state then gives the eigenvalues ω and σ, the frequency and growth rate of the wavy modes. These eigenvalues must be calculated for all the relevant values of m; they are found using the methods described in paper I.

3. Small disturbances to the azimuthal flow

Krueger *et al.* (1966) discovered that for μ sufficiently negative, non-axisymmetric disturbances to the azimuthal flow can grow at a lower Taylor number than axisymmetric disturbances. The value of μ below which this occurs is a function of η, the radius ratio; it is therefore possible to divide the (η, μ)-plane into regions where the critical disturbance is axisymmetric or non-axisymmetric. In order to decide on which side of the dividing curve a point in the (η, μ)-plane lies we have to perform the following procedure. For each m, including $m = 0$, we must find the axial wavenumber α_m, which gives minimum critical Taylor number Ta_m.

The critical value of m is that value which gives smallest Ta_m; if this is $m = 0$ the point (η, μ) lies above the dividing curve; if it is $m \neq 0$, the point lies below. So on the dividing curve the smallest Ta_m, $m \neq 0$, equals Ta_0.

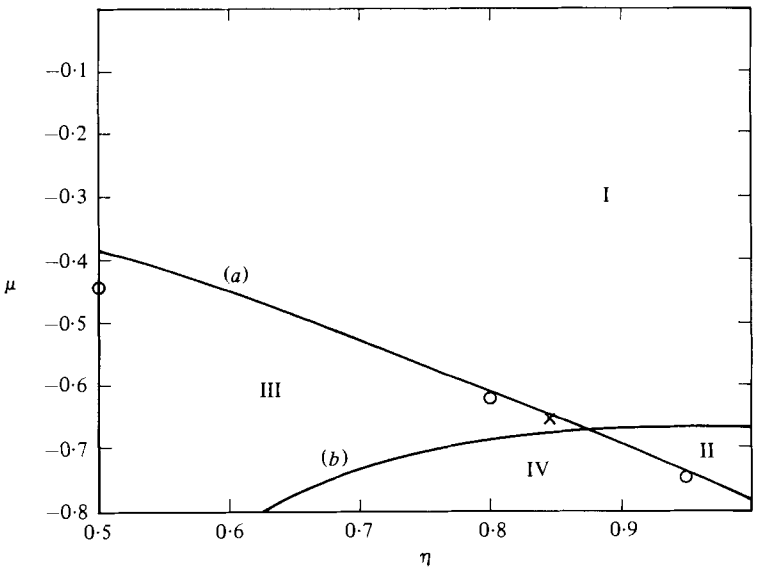

FIGURE 1. The (η, μ)-plane is divided into four regions by (*a*) the curve on which disturbances with $m = 0$ and $m = 1$ have neutral stability at the same Taylor number, and (*b*) the curve above which the axisymmetric disturbances are supercritical and below which they are subcritical.

The computer program actually calculates the growth rate σ as a function of Ta, μ, η, α and m, so $\sigma = \sigma(Ta, \mu, \eta, \alpha, m)$. If μ, η and m are fixed, then $\sigma(Ta, \alpha) = 0$ defines the curve of critical Ta as a function of α. Minimum critical Taylor number occurs when $dTa/d\alpha = 0$; since $d\sigma = (\partial\sigma/\partial Ta)\,dTa + (\partial\sigma/\partial\alpha)\,d\alpha = 0$ on the curve $\sigma = 0$, minimum critical Taylor number occurs when $\partial\sigma/\partial\alpha = 0$. So a point where $Ta_m = Ta_0$ will satisfy the four nonlinear simultaneous equations

$$\left.\begin{aligned} \sigma(Ta, \mu, \eta, \alpha_m, m) &= 0, \\ \frac{\partial\sigma}{\partial\alpha}(Ta, \mu, \eta, \alpha_m, m) &= 0, \\ \sigma(Ta, \mu, \eta, \alpha_0, 0) &= 0, \\ \frac{\partial\sigma}{\partial\alpha}(Ta, \mu, \eta, \alpha_0, 0) &= 0. \end{aligned}\right\} \tag{3.1}$$

If η and m are chosen, these equations can be solved for the four unknowns Ta, μ, α_0 and α_m using Newton–Raphson iteration. In the range $0{\cdot}5 \leqslant \eta < 1$ it was found that the $m = 1$ mode gave the minimum critical Taylor number on the dividing curve. Since the azimuthal flow state is ζ-independent, disturbances are proportional to $\exp(i\alpha\zeta)$, so we can truncate expansions of the form (2.3) or (2.4) at $N = 1$. Since $M = 16$ gives accurate solutions for values of μ and η in the range under consideration, each evaluation of σ takes only a very short time; furthermore, since the Newton–Raphson procedure iterates on all four unknowns simultaneously each point on the curve can be obtained reasonably quickly. The dividing curve is shown in figure 1 as curve (*a*). The values of α_0 and α_m are not very different; at $\eta = 0{\cdot}5$, $\mu = -0{\cdot}39$, $Ta = 15{\cdot}45 \times 10^3$, $\alpha_0 = 4{\cdot}08$ and $\alpha_1 = 3{\cdot}81$, and for narrow gaps α_0 and α_1 become much closer together. This dividing curve is important for our study, since it is only

above this curve that axisymmetric vortices occur; our method is therefore only applicable to that part of parameter space lying above the dividing curve. Also plotted in figure 1 are the experimental points of Snyder (1968) and Nissan *et al.* (1963). They also found $m = 1$ to be the critical m. Agreement is reasonably good for the points with $\eta \geqslant 0{\cdot}8$; the $\eta = 0{\cdot}5$ point is, however, significantly out.

DiPrima & Grannick (1971) showed that finite-amplitude Taylor vortices can exist at a lower Taylor number than critical in certain regions of the (η, μ)-plane. For subcritical instability it is necessary to have μ sufficiently negative, so we again have a dividing curve in the (η, μ)-plane. Above this curve, which is labelled (*b*) in figure 1, Taylor vortices are supercritical, below it they are subcritical. This curve was constructed using the nonlinear Taylor-vortex program; at given μ and η a nonlinear solution was found for Ta slightly above Ta_{v}. Then Ta was reduced while the amplitude of the solution was monitored. In a supercritical case the amplitude tends to zero as this is done, while in a subcritical case the amplitude tends to some finite value. In this way we can bracket the dividing curve and hence construct it. This procedure would be rather inefficient if it were not for the fact that near critical Ta only the second-harmonic and mean-motion terms are stimulated; we can therefore use our nonlinear program truncated at $N = 2$. We should note, however, that to determine the minimum value of Ta at which subcritical motion occurs it is not sufficient to set $N = 2$.

The two curves in figure 1 divide the (η, μ)-plane into four regions: I, II, III and IV. in region I we have supercritical Taylor-vortex flow, that is as Ta is increased from small values an axisymmetric transition is followed by the smooth development of Taylor vortices. In many cases these vortices subsequently become wavy. In region II we have subcritical Taylor-vortex flow; an axisymmetric transition takes place, but it is followed by a jump to finite-amplitude vortices. Subsequent lowering of Ta leads to hysteresis, since steady vortices are possible for $Ta < Ta_{\mathrm{v}}$. In region III non-axisymmetric modes will develop first, so the motion immediately becomes fully three-dimensional. In region IV the axisymmetric transition is subcritical, but non-axisymmetric modes have a lower Ta_{c} than axisymmetric modes; the expected behaviour cannot therefore be predicted without further calculation.

In this paper we shall concentrate on region I; however, some investigation of subcritical Taylor vortices was made. The situation here resembles that in penetrative convection (Veronis 1963; Musman 1968; Moore & Weiss 1973). The x-value corresponding to zero azimuthal velocity is given by

$$x_{\mathrm{n}} = \frac{\eta}{1-\eta}\left[\left(\frac{1-\mu}{\eta^2-\mu}\right)^{\frac{1}{2}} - 1\right] \tag{3.2}$$

in the Couette-flow solution, and the angular momentum distribution is stable for values of x satisfying $x_{\mathrm{n}} < x < 1$. It is convenient to introduce a Taylor number and wavenumber based on the width of the unstable region only:

$$Ta' = x_{\mathrm{n}}^4 Ta, \quad \alpha' = \alpha x_{\mathrm{n}}. \tag{3.3}$$

The behaviour of subcritical Taylor vortices is then closely analogous to the behaviour of two-dimensional penetrative convection as described by Moore & Weiss (1973).

The coefficients a_{mn}

n \ m	0	1	2	3	4	5	6
0	1019·4	−132·9	23·8	−2·6	1·0	−0·1	−0·1
1	623·0	−130·0	31·5	−7·9	0·1	−0·1	0·2
2	358·1	−163·9	14·7	−3·2	2·1	−0·2	−0·1
3	156·0	−139·4	32·4	−1·3	−0·6	−0·5	0·2
4	56·6	−65·6	28·6	−8·8	0·6	0·6	−0·1
5	18·3	−21·4	9·0	−5·0	2·5	−0·3	−0·2
6	6·9	−8·7	2·0	0·6	0·0	−0·7	0·4
7	3·9	−6·2	3·3	−0·8	−0·2	0·0	0·1
8	1·6	−2·7	2·1	−1·4	0·5	0·2	−0·2

The coefficients b_{mn}

n \ m	0	1	2	3	4	5	6
0	2·3036	0·0864	−0·0008	0·0037	0·0014	−0·0005	−0·0003
1	0·5208	0·0869	−0·0091	−0·0066	−0·0033	0·0010	0·0006
2	0·2502	−0·1004	−0·0245	0·0067	0·0042	−0·0004	−0·0008
3	0·0613	−0·0893	0·0304	0·0057	−0·0054	−0·0008	0·0011
4	0·0041	−0·0059	0·0175	−0·0139	0·0018	0·0019	−0·0006
5	−0·0035	0·0103	−0·0097	0·0001	0·0046	−0·0013	−0·0007
6	0·0013	−0·0011	−0·0038	0·0071	−0·0043	−0·0005	0·0012
7	0·0019	−0·0036	0·0031	−0·0010	−0·0011	0·0007	0·0001
8	0·0001	−0·0006	0·0015	−0·0026	0·0021	−0·0001	−0·0005

TABLE 1

As μ is decreased from 0, Ta' starts to fall, owing to the 'softening' of the outer boundary condition. After some small oscillation, Ta' eventually flattens out to 591 at large negative μ for all values of η (Chandrasekhar 1961). In the narrow-gap case the motion becomes subcritical at $\mu \simeq -0{\cdot}7$; Musman (1968) gives the corresponding parameter in penetrative convection, $1-\lambda$, as $\simeq -0{\cdot}8$. As μ is further reduced, counter-cells appear, the first counter-cell appearing in the neighbourhood of $\mu \simeq -0{\cdot}9$; Moore & Weiss (1973) find counter-cells appearing when $1-\lambda < -0{\cdot}91$ in penetrative convection.

In comparing experiment with theory the critical Taylor number and axial wavenumber are often found; for example the experiments of Donnelly & Fultz (1960) were satisfactorily compared with the calculations of Chandrasekhar (1958). Since Ta_{v} and α_{c}, the critical wavenumber at the onset of Taylor vortices, are fundamental to these calculations, in table 1 information is given which enables these quantities to be evaluated with the aid of a programmable calculator, for the range $0{\cdot}5 \leqslant \eta < 1$ and $-0{\cdot}8 \leqslant \mu \leqslant 0$. We write

$$Ta'_{\mathrm{v}} = \sum_{m=0}^{m=6} \sum_{n=0}^{n=8} a_{mn}\, T_m(\eta^*)\, T_n(\mu^*), \tag{3.4}$$

$$\alpha'_{\mathrm{c}} = \sum_{m=0}^{m=6} \sum_{n=0}^{n=8} b_{mn}\, T_m(\eta^*)\, T_n(\mu^*), \tag{3.5}$$

where $\eta^* = 4(\eta - 0{\cdot}75)$, $\mu^* = 2{\cdot}5(\mu + 0{\cdot}4)$, and Ta' and α' are given by (3.3). T_m and T_n are the mth and nth Chebyshev polynomials respectively. The values of a_{mn} and b_{mn}

η	μ	Ta_e	α_e	Ta_1	α_1	Ta_1'	α_1'
0·6	−0·3	5710·1	3·294	5712·8	3·291	766·3	1·992
0·6	−0·7	27 359	5·006	27 350	5·004	697·4	2·000
0·9	−0·3	2719·2	3·161	2718·7	3·160	814·6	2·338
0·9	−0·7	6406·7	3·514	6404·4	3·511	583·7	1·929

TABLE 2

are listed in table 1. Ta_v' and α_c' have a smaller range of values than the original variables Ta_v and α_c, which means that fewer coefficients are required to give a desired accuracy.

Ta_v' and α_c' can easily be found from table 1 using an adapted form of Clenshaw's (1955) method (see e.g. Hildebrand 1956). We define $c_{8n} = c_{7n} = 0$ and then use the recurrence relation

$$c_{mn} = 2\eta^* c_{m+1,n} - c_{m+2,n} + a_{mn}, \tag{3.6}$$

to evaluate c_{0n} and c_{1n}. We then define $e_{10} = e_9 = 0$ and $d_n = c_{0n} - \eta^* c_{1n}$, and use

$$e_n = 2\mu^* e_{n+1} - e_{n+2} + d_n, \tag{3.7}$$

to evaluate $Ta_v' = e_0 - \mu^* e_1$. To evaluate α_c' we again set $c_{8n} = c_{7n} = e_{10} = e_9 = 0$ and use (3.6), but this time we put the b_{mn} coefficients in instead of the a_{mn} coefficients. Then we use (3.7) as before to obtain $\alpha_c' = e_0 - \mu^* e_1$. The values of α and Ta can then be found from (3.2) and (3.3).

In table 2 we give the results obtained by using table 1 to compute selected values of Ta_v and α_c; these values are listed as Ta_1 and α_1 in table 2. We also give the corresponding Ta_v' and α_c' (see (3.3)) listed as Ta_1' and α_1'. We can compare these results with the 'exact' values of Ta_v and α_c computed by full numerical integration, and labelled Ta_e and α_e in table 2.

From this table we can see that the errors incurred by using table 1 rather than full numerical integration are generally about 0·1 %.

4. Nonlinear axisymmetric Taylor-vortex solutions

In regions I and II of figure 1 we know that the first transition from azimuthal flow will be axisymmetric. It is therefore natural to find nonlinear axisymmetric solutions in these regions and to test their stability to axisymmetric and non-axisymmetric perturbations. A well-known problem lies in deciding on the appropriate choice of α, the axial wavenumber, in the nonlinear regime. This problem has been considered both experimentally (e.g. Coles 1965; Snyder 1969*a*; Donnelly & Schwarz 1965) and theoretically (e.g. DiPrima & Eagles 1977). The presence of end walls means that a discrete number of cells N has to fit in the apparatus, and all experiments indicate that several different values of N are possible. In the experiments there is therefore a set of discrete attainable axial wavelengths lying in a band.

The simplest strategy is to adopt that value of $\alpha = \alpha_c$ which minimizes Ta_v, and assume that α does not change as Ta is increased. This procedure gives good agreement with observation in the case $\mu = 0$ (see paper I); in this case the experimentally

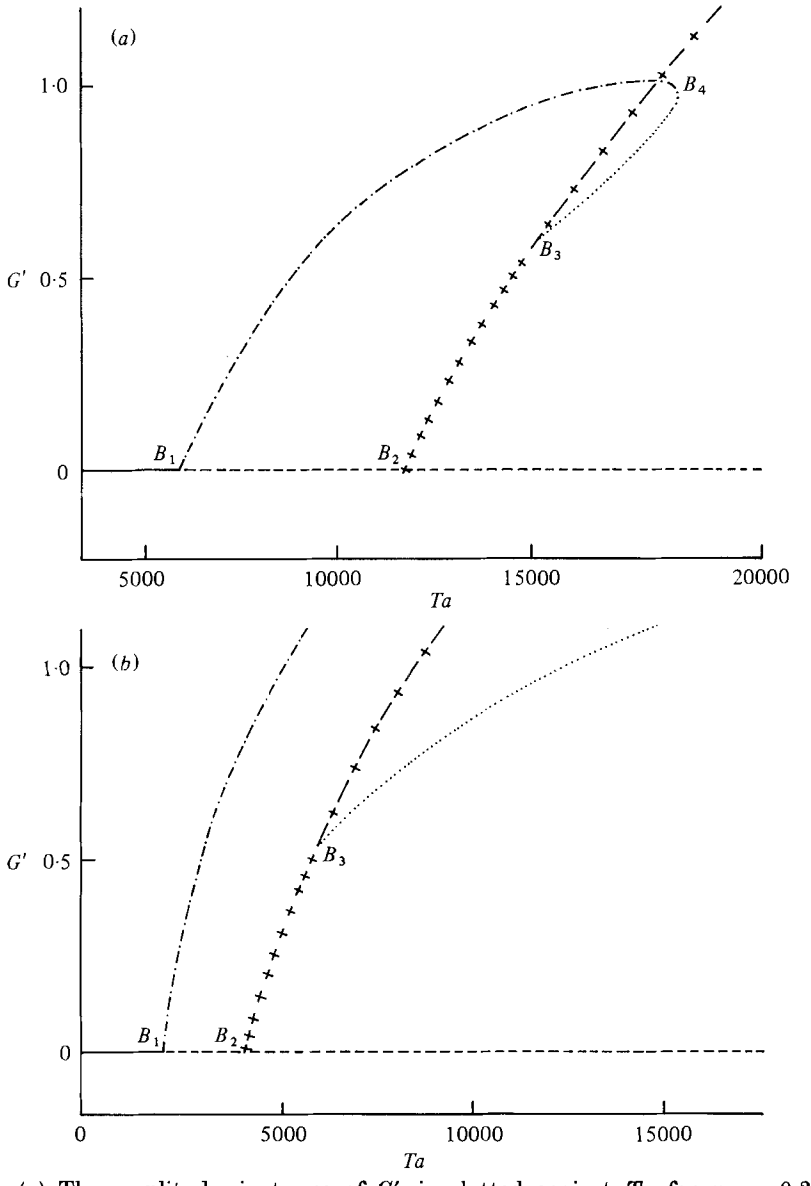

FIGURE 2. (*a*) The amplitude, in terms of G', is plotted against Ta for $\mu = -0{\cdot}2$, $\eta = 0{\cdot}5$; ——, stable Couette-flow solution; – – –, unstable Couette-flow solution; –·–·–, stable primary solution, wavenumber $\alpha_c = 3{\cdot}27$; · · · · ·, unstable alternating-cell solution, wavenumber α_c; – × – × –, stable secondary solution, wavenumber $2\alpha_c$; × × × ×, unstable secondary solution, wavenumber $2\alpha_c$. (*b*) The amplitude, in terms of G', is plotted against Ta for $\mu = 0$, $\eta = 0{\cdot}8756$: ——, stable Couette-flow solution; – – –, unstable Couette-flow solution; –·–·–, stable primary solution, wavenumber $\alpha_c = 3{\cdot}13$; · · · · ·, unstable alternating-cell solution, wavenumber α_c; – × – × –, stable secondary solution, wavenumber $2\alpha_c$; × × × ×, unstable secondary solution wavenumber $2\alpha_c$.

observed band of results usually includes α_c. As we shall see, this choice of α unfortunately cannot always be extended to the case where μ is non-zero.

We should note that the axisymmetric solutions become unstable to non-axisymmetric disturbances in some regions of the (η,μ)-plane; however, it is still of interest to study the purely axisymmetric problem, as it can be useful to view some parts of the wavy-vortex regime as a basic axisymmetric flow with a small non-axisymmetric component superimposed.

After the first transition, the amplitude of axisymmetric vortices can be conveniently measured in terms of $G' = (G-G_a)/G_0$, where

$$G = G_0\left[\frac{2(1-\mu)}{\eta(1+\eta)} - \left.\frac{\partial v}{\partial x}\right|_{x=0}\right], \tag{4.1}$$

is the torque on the inner cylinder, $(\partial v/\partial x)|_{x=0}$ being the average value over ζ. $G_a = 2(1-\mu)G_0/\eta(1+\eta)$ is the torque of the azimuthal flow solution, and

$$G_0 = 2\pi R_1^3 h\nu\rho\Omega_1/d, \tag{4.2}$$

where h is the length of the cylinders and ρ is the fluid density. We should note that G' increases as the square of the Taylor-vortex flow in the neighbourhood of Ta_c.

In figure 2 we have plotted G' against Ta for the two cases (*a*) $\eta = 0{\cdot}5, \mu = -0{\cdot}2$ and (*b*) $\eta = 0{\cdot}8756, \mu = 0$. Also we have indicated which solutions are unstable to axisymmetric disturbances and which are stable to such disturbances. Only those solutions with wavenumber α_c, or multiples of α_c, are shown in the figures. Figure 2 has been constructed using a comparatively severe truncation with $N = 4$; the topology of the pictures is the same at higher values of N, but the actual values of G' are a few per cent lower. At large Taylor numbers there are several different solutions at the same value of Ta; the solution obtained on any one run depends on the starting values of the iterative procedure. It is not possible to be certain in advance to which solution any particular starting value will lead to; an unstable solution is just as likely to be found as a stable one, so for example the solution $\psi = v = 0$, the Couette-flow solution, can be found at any value of Ta. Also, solutions that have $\psi_{mn} = 0$ for odd n and $v_{mn} = 0$ for even n can sometimes be found; from (2.2) and (2.3) we can see that these correspond to solutions with period 2α as well as α. Similarly, solutions with period $n\alpha$, for any integer n can be found, provided that the truncation number N and the Taylor number are large enough.

Given the non-uniqueness of the solutions it is legitimate to ask whether all the solutions of period α have been found. It is not possible to give a definite answer to this; however, by examining the axisymmetric stability of the solutions that have been found we can see that there are no other solutions bifurcating from those we have calculated, since points of bifurcation will only occur at points where neutrally stable disturbances exist. We can therefore be reasonably sure that all solutions that can be continuously traced back to the Couette-flow solution have been found. Since it is only stability or instability to axisymmetric solutions that helps us sort out the topology of nonlinear axisymmetric solutions, in this section we shall assume the word 'axisymmetric' qualifies the words 'stable' and 'unstable'. Non-axisymmetric stability will be considered in § 5.

Since figure 2 is more complicated than we might have expected, some explanation is required. Consider figure 2(*a*) first. The Couette-flow solution is the only one when

$Ta < Ta_v = 5885$; the primary solution bifurcates from this solution at the point B_1 with wavenumber $\alpha_c = 3{\cdot}266$. This stable solution increases in amplitude smoothly at first as Ta is increased. From $5885 < Ta < 11632$ this branch is the unique non-trivial solution with wavelength $2\pi/\alpha_c$. At $Ta = 11632$ a secondary solution with wavenumber $2\alpha_c$ bifurcates from the (unstable) Couette-flow solution at B_2. This 'double-roll' secondary solution with wavenumber $2\alpha_c$ is initially unstable to disturbances of wavenumber α_c. As Ta is further increased this secondary solution bifurcates at $Ta \simeq 15000$, the point labelled B_3 in figure 2(*a*). Two branches emerge, one of which is still a double-roll solution, which now becomes stable, but the other has period $2\pi/\alpha_c$ but not π/α_c. In this new solution, called the alternating-cell solution in figure 2(*a*), one of the double rolls is strengthened while the other is weakened. As Ta is increased further, the amplitudes of the even multiples of α_c weaken, while the amplitudes of the odd multiples strengthens. Finally, at $Ta \simeq 18800$, at the point labelled B_4, this unstable alternating-cell solution joins onto the primary solution that bifurcated at B_1. So the primary solution no longer exists when $Ta > 18800$. It should be noted that there will be other solutions of period $2\pi/3\alpha_c$, $2\pi/4\alpha_c$ etc. bifurcating from the azimuthal solution. The development of these solutions was not examined in this study.

There is another point to be mentioned in connection with figure 2: at the bifurcation points B_1, B_2 and B_3 there are shown just three solutions meeting at each of these points. For example, at B_1 we have the stable Couette-flow solution, the unstable Couette-flow solution and the primary solution. In some sense, however, there are really two primary solutions, one with the outgoing jet centred on $\zeta = 0$ and one with the return flow centred on $\zeta = 0$. Of course, in the infinite-cylinder geometry these two solutions are identical, since one is just the other displaced by π/α along the ζ-axis. However, as emphasised by Benjamin & Mullin (1980), if the translational symmetry in the axial direction is removed by the presence of end walls, then in general these two solutions are no longer identical, and so we have four solutions meeting at each bifurcation. This degeneracy also occurs at B_2 and B_3. In the case of B_3, it is the alternating-cell solution that should be counted twice; if we consider any particular adjacent pair of rolls in the double-cell solution these can either strengthen or weaken (see figure 3*c*, *d*), so two alternating-cell solutions develop. In our translationally symmetric problem (no end effects) these two solutions are identical, and so only appear as one in figure 2.

To illustrate the above discussion, and the physical nature of the various solutions shown in figure 2(*a*), the streamlines and contours of equal azimuthal velocity are plotted in figure 3 for four points in figure 2(*a*). The four points are: (*a*) the primary solution at $Ta = 8000$; (*b*) the primary solution at $Ta = 18000$; (*c*) the alternating-cell solution at $Ta = 18000$; (*d*) the secondary 'double-roll' solution at $Ta = 14000$. In all eight drawings, the left-hand edge is at the inner cylinder and the right-hand edge is at the outer cylinder. From these pictures we can gain some insight into why the primary solution develops into the alternating-cell solution at the 'nose' of the curve, the point B_4. As we pass from 3(*a*) to 3(*b*) we can see from the streamlines that the outgoing jet from the inner cylinder is becoming narrower and faster, while the return flow becomes broader and weaker. Even in the $\mu = 0$ case, the outgoing jet attains higher speeds than the return flow (see paper I) but in the counter-rotating case this effect is further enhanced. A similar feature is the fast narrow rising plume and

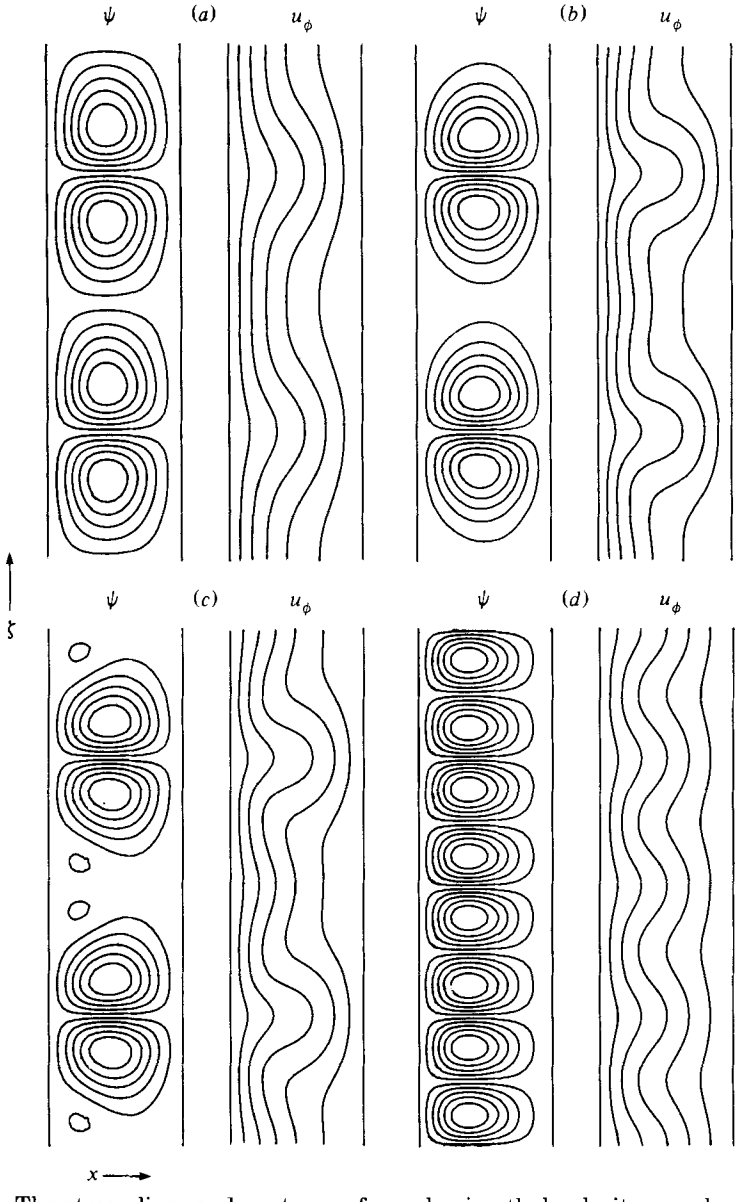

FIGURE 3. The streamlines and contours of equal azimuthal velocity are shown for four cases with $\mu = -0{\cdot}2$, $\eta = 0{\cdot}5$. (*a*) Primary solution, $Ta = 8000$, $\alpha = 3{\cdot}27$. (*b*) Primary solution, $Ta = 18000$, $\alpha = 3{\cdot}27$. (*c*) Alternating-cell solution, $Ta = 18000$, $\alpha = 3{\cdot}27$. (*d*) Secondary solution, $Ta = 14000$, $\alpha = 6{\cdot}53$.

broader descending region which occurs in two-dimensional penetrative convection (Moore & Weiss 1973). A consequence of this asymmetry is that the lines of equal azimuthal velocity, and hence of equal angular momentum, are relatively undisturbed in the region occupied by the return flow (see figure 3*b*). So in this region there is a comparatively small distortion of the angular momentum distribution from its Couette-flow value. But at $Ta > 11632$ this angular momentum distribution is

unstable to distances of wavenumber $2\alpha_c$; the small distortion of the return flow can delay the onset of instability of the primary solution to disturbances of wavenumber $2\alpha_c$ to $Ta = 18800$ but no further. So at the point B_4 the primary solution is neutrally stable to disturbances of wavenumber $2\alpha_c$. These considerations, do not, however, explain why the primary solution joins onto the alternating-cell solution rather than, for example, bifurcating into an unstable primary solution and a stable alternating-cell type of solution.

Figure 2 (*b*), the $\mu = 0$ case, behaves similarly except in one vital respect: the primary solution (this time bifurcating at $Ta_v = 1860$) does not join up with the solution bifurcating from the double-roll solution. It is of course possible that these solutions do join up at a higher value of Ta than the present numerical schemes allow; from the present work we can say that this does not happen for $Ta < 25\,Ta_v$. Recently Booz (1980) has found the primary solution up to $Ta \simeq 100\,Ta_v$ using finite-difference methods. So it appears likely that for $\mu = 0$ the primary solution exists at least as far as the onset of the turbulent regime. The solution bifurcating from the double-roll solution at the point B_3 is of the alternating cell form. At large Ta, the weaker roll becomes very small, while the larger cell resembles that of the primary solution.

What is the solution to the dilemma posed by the disappearance of the primary solution in figure 2 (*a*)? There appear to be two possibilities: (i) the primary solution has become unstable to non-axisymmetric modes before $Ta = 18800$ and a wavy-vortex regime exists beyond $Ta = 18800$ where an axisymmetric vortex cannot exist; or (ii) the wavenumber α_c is no longer in the stable range and the wavelength has to shorten. For $\eta = 0{\cdot}5$ and $\mu = -0{\cdot}2$ case (ii) is to be preferred on both experimental and theoretical grounds. Snyder (1969*a*) finds that in this region of the (η, μ)-plane the centre of the band of allowed wavelengths decreases as Ta increases, and that α_c does not stay in the band as Ta increases. On the theoretical side, the axisymmetric solution with $\alpha = \alpha_c$ was found to be stable to non-axisymmetric disturbances, further reducing support for the first possibility.

It therefore appears possible that the upper bound on permissible wavelengths in the Snyder experiments is set not just by stability considerations, but by the non-existence of equilibrium solutions. The lower bound, however, must be set by stability considerations, because the solution with $\alpha = 2\alpha_c$ is outside the range of wavenumber observed by Snyder.

It was not possible to plot pictures similar to figure 2 all over the (η, μ)-plane. However, at $\eta = 0{\cdot}9, \mu = -0{\cdot}7$ a picture very similar to that of figure 2 (*a*) was found, with the 'nose' occurring at about $Ta \simeq 24000$, so this behaviour probably occurs over a large area of the (η, μ)-plane of figure 1. The effect of increasing α somewhat above α_c was also investigated; fairly small increases in α led to a rapid increase of the Ta-value of the nose. So increasing α by the amount observed by Snyder removes the difficulty and allows us to find axisymmetric solutions at large Ta.

5. Stability of nonlinear axisymmetric solutions

Since it was not practical to investigate the stability of the nonlinear solutions over the whole of the (η, μ)-plane, three aspects were singled out for particular attention.

The first question concerns the wavy vortices observed for narrow gaps. How does the onset of waviness vary as μ becomes negative? The solution to this is displayed in

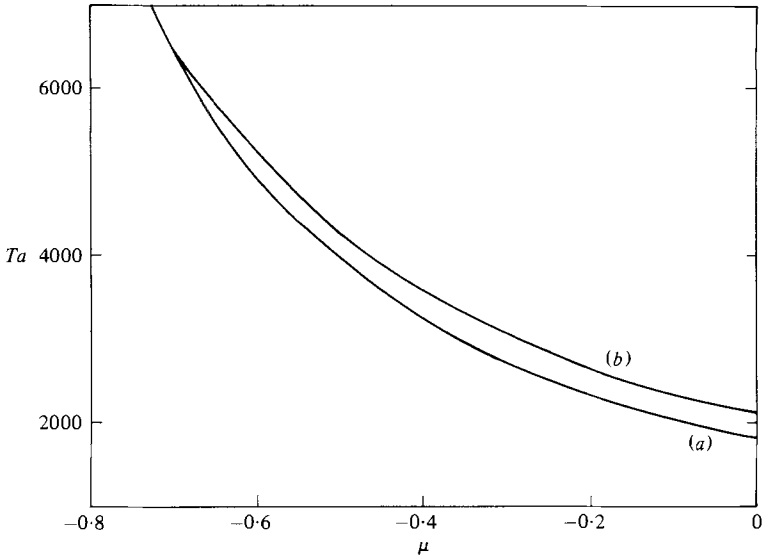

FIGURE 4. The Taylor number Ta_v for the onset of axisymmetric modes against μ is curve (a). The Taylor number Ta_w for the onset of waviness is curve (b). The gap ratio $\eta = 0{\cdot}9$.

figure 4. The lower curve is the Taylor number Ta_v at the onset of axisymmetric motion. This curve is constructed by considering $m = 0$ disturbances about the state of circumferential Couette flow. The same expansion method as described in § 2 was used to calculate this curve, but since the basic state is purely azimuthal, only the $n = 1$ term in the ζ-expansion needs to be considered. The upper curve is the Taylor number Ta_w for the onset of out-of-phase wavy modes. This curve is calculated by perturbing the nonlinear Taylor-vortex flow, and so requires the full ζ-expansion; $m = 1$ is the first mode to become unstable throughout this range. The two curves merge near $\mu = -0{\cdot}7$; at this point the $m = 1$ and $m = 0$ modes become unstable simultaneously (see figure 1). The analogous curve for the narrow-gap limit was obtained by Nakaya (1975), using the amplitude-expansion method; figure 4 was obtained using $\eta = 0{\cdot}9$. Our results are in good agreement with his; this is not surprising since Ta_w is just above Ta_v throughout the range $-0{\cdot}7 < \mu < 0$, so we would expect the amplitude-expansion method to give good results. Stability to in-phase modes was also tested at various points in the range; non-axisymmetric in-phase modes were always found to be more stable than axisymmetric in-phase modes.

The second area of investigation was comparison with Snyder's (1969*a*, *b*) results with $\eta = 0{\cdot}5$. It was found in paper I that at $\mu = 0$ Taylor vortex flow is stable up to at least $Ta < 30000$ when $\eta = 0{\cdot}5$; it is also observed experimentally that the usual wavy mode does not occur here (Snyder 1969*a*, *b*; K. J. Park 1980 private communication). The unstable wavy mode was found when μ becomes negative, however, in accord with Snyder's observations.

As explained in § 4, it is no longer adequate to leave α fixed at α_c; we must consider a range of α with $\alpha > \alpha_c$. This is, of course, more expensive computationally, so the point $\eta = 0{\cdot}5$, $\mu = -0{\cdot}2$ was fixed on; it lies comfortably in the middle of the range considered by Snyder. We find here that $m = 2$ is the strongly preferred mode, as did Snyder in his experiments; indeed, it was this strong preference that motivated Snyder

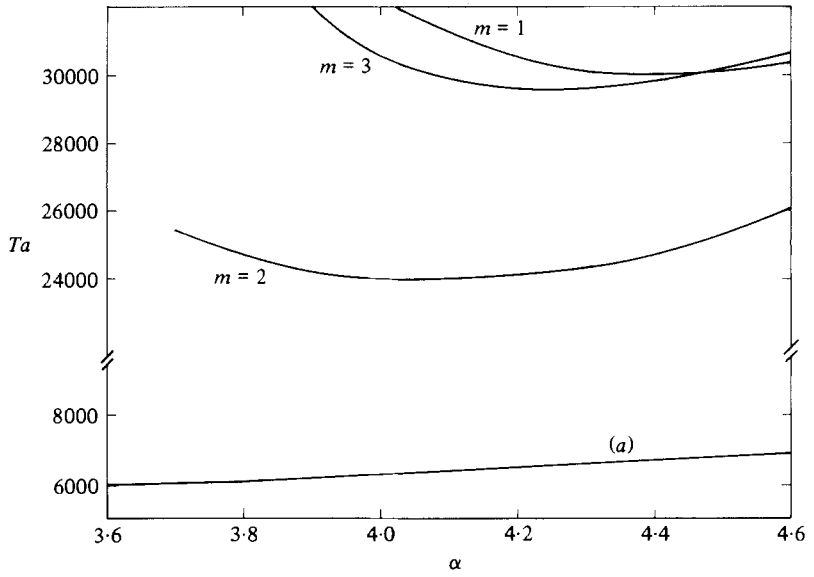

FIGURE 5. Ta_w for the wavy modes $m = 1$, 2 and 3 is plotted against α, the axial wavenumber, for $\mu = -0{\cdot}2$ and $\eta = 0{\cdot}5$. Curve (a) is the onset of Taylor vortices Ta_v for the same case.

to examine this region of the (η,μ)-plane. In figure 5 we have plotted the values of Ta_w, the Taylor number at the onset of waviness, against α for $m = 1$, 2 and 3. The $m = 2$ mode becomes unstable at a Taylor number several thousands below that of either $m = 1$ or $m = 3$. This is rather unusual behaviour; the wavy narrow-gap modes usually have $m = 1$ unstable first, but quickly followed by $m = 2$ and then larger m-values. Each point on the curves needs a new nonlinear axisymmetric state to be calculated, as this varies with α. The curve ends at $\alpha \simeq 3{\cdot}7$ because no singly periodic steady-state solution could be found for smaller α (see §4). Also shown in figure 5 is the curve of Ta_v, the critical Taylor number for the onset of Taylor vortices, against α. The minimum value of Ta_v is off the picture, which is why Ta_v increases monotonically with α in figure 5.

Snyder found that for his apparatus the onset of the $m = 2$ wavy mode was $\Omega_1 d^2/\nu = 146$, which for $\mu = -0{\cdot}2$ and $\eta = 0{\cdot}5$ implies $Ta_w = 25600$. This experimental value was the smallest value obtained over many observations with different numbers of vortices in the apparatus (Snyder 1969*b*). The fairest comparison is therefore to take the minimum theoretical value as α varies; from figure 4 this gives $Ta_w = 24000$. The comparatively small difference is probably due to the experiments having endwalls, while the theory is for infinite cylinders. Snyder also gives the frequency of the wavy mode for a wide range of Ta and μ. Agreement here between theory and experiment seems reasonably satisfactory for cases near the stability boundary; for example, at $Ta = 30720$, $\alpha = 3{\cdot}85$, $\omega d^2/\nu$ was computed to be 11·8, while Snyder's experiment gives just over 13 (see Snyder 1969*b*, figure 7).

As Ta is increased, however, the observed frequencies are systematically larger than the computed linear frequencies. This is perhaps not surprising, as the computations are ignoring nonlinear effects due to the waves themselves; these clearly can, and apparently do, affect the wave frequencies. It is worth noting, however, that the linear

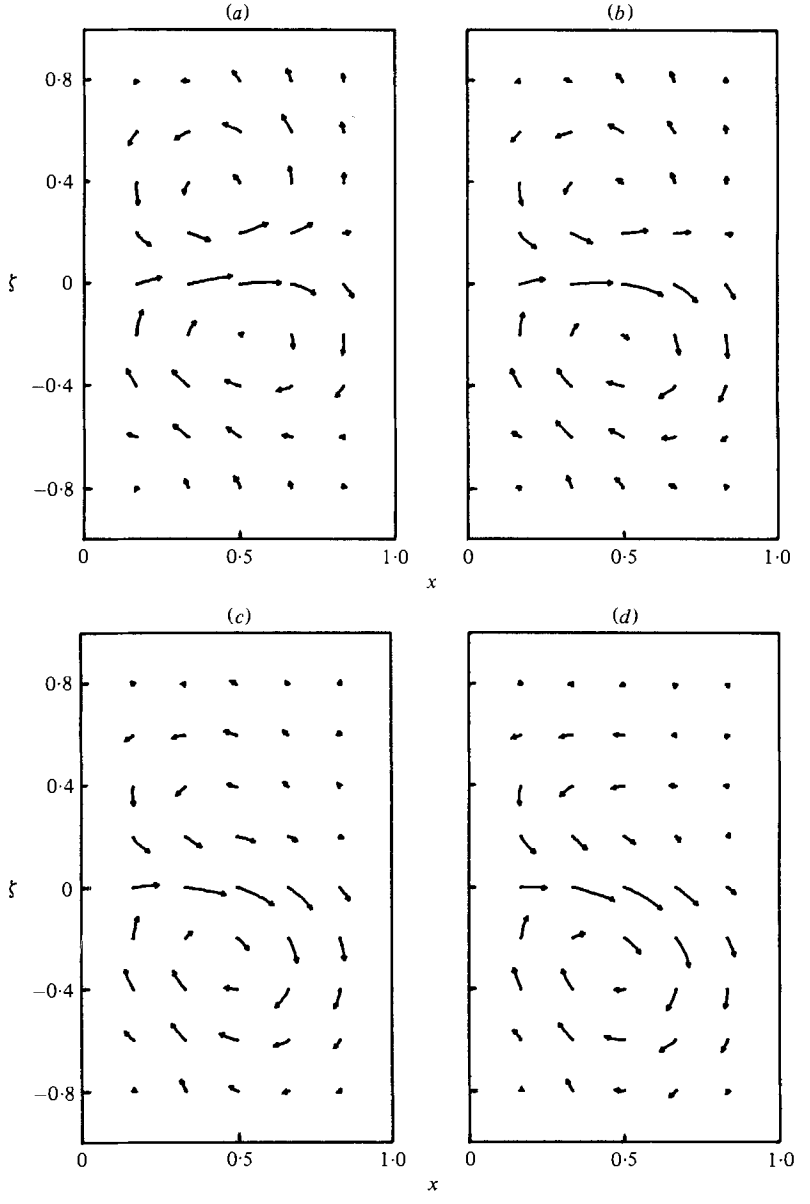

FIGURE 6. A quarter-period of the waveform $m = 2$ in the (x, ζ)-plane; $Ta = 32400$, $\alpha = 3{\cdot}85$; $\mu = -0{\cdot}2$, $\eta = 0{\cdot}5$.

theory gave good agreement with observed frequencies at Ta well above Ta_w in the fixed-outer-cylinder case.

Snyder also gives details of the waveform in the (r, z)-plane (1969*b*). To facilitate comparison with Snyder's description of the waveform, figure 6 has been constructed. The radial and axial velocities u_r and u_z were found for the nonlinear axisymmetric solution corresponding to $Ta = 32400$ and $\alpha = 3{\cdot}85$ on a mesh in the (x, ζ)-plane. The unstable $m = 2$ disturbance was computed and the u_r and u_z components found for the (x, ζ)-planes $\phi = 0$, $\frac{1}{6}\pi$, $\frac{1}{3}\pi$ and $\frac{1}{2}\pi$. A certain percentage of the disturbance field is

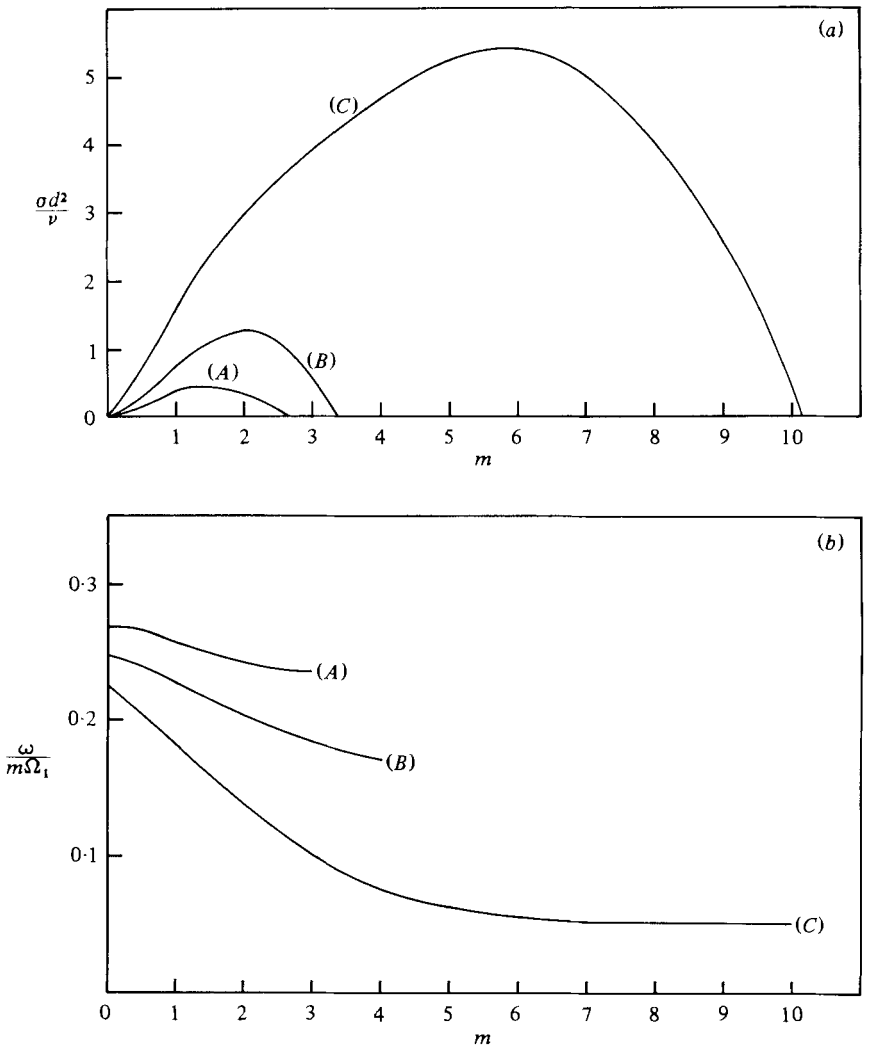

FIGURE 7. (*a*) The growth rate is shown as a function of m, the azimuthal wavenumber for the case $\mu = -0{\cdot}6$, $\eta = 0{\cdot}8756$, $\alpha_c = 3{\cdot}37$. Curves for $Ta = 1{\cdot}21\ Ta_v$ (*A*), $Ta = 1{\cdot}44\ Ta_v$ (*B*), and $2{\cdot}25\ Ta_v$ (*C*) are shown. (*b*) The phase speed $\omega/m\Omega_1$ as a function of m, the azimuthal wavenumber for the case $\mu = -0{\cdot}6$, $\eta = 0{\cdot}8756$ and $\alpha_c = 3{\cdot}37$. The Taylor numbers of the three curves are the same as in figure 7(*a*).

then added to the axisymmetric field; the four resulting fields are displayed in figure 6, in which the arrows have x- and ζ-components proportional to u_r and u_z, so that the length of arrows is proportional to $(u_r^2+u_z^2)^{\frac{1}{2}}$. The percentage of disturbance that is added is to some extent arbitrary; in constructing figure 6 the maximum radial disturbance speed u_r' at $\phi = 0$ is 13 % of the maximum radial speed of the axisymmetric jet. The four pictures (*a*), (*b*), (*c*) and (*d*) represent $\frac{1}{4}$ of the cycle of the wave. The rest of the first half of the cycle consists of reversing the sequence, so we have (*d*), (*c*), (*b*) and finally (*a*). In the remaining half of the cycle the outgoing jet swings upward, and the sequence is a mirror image of the first part of the cycle. The downturn of the jet at the beginning of the cycle, the strengthening of the lower cell and the diminishing of

the upper cell, and the fact that the outgoing jet at the inner cylinder moves very little in space throughout the cycle are the main features noted by Snyder, and all can be seen in the sequence shown in figure 6.

The third area of investigation was at $\eta = 0{\cdot}8756$ and $\mu = -0{\cdot}6$. The purpose of this was to examine frequencies and growth rates as functions of the wavenumber m, and to compare them with the results previously obtained at $\mu = 0$. The growth rate as a function of m is shown in figure 7 (a) for a variety of Taylor numbers. The growth rates behave similarly to those in the $\mu = 0$ case; there is a gradual move of the fastest growing m-mode to higher wavenumbers as Ta increases. Because of the uncertainty about the value of α, we have not gone beyond $Re = 1{\cdot}5\, Re_{\text{crit}}$. In figure 7 ($b$) we show the frequencies; these are substantially different from the $\mu = 0$ case, particularly at the higher values of Ta. In the $\mu = 0$ case, $\omega/m\Omega_1$, the phase speed, is approximately independent of m at all values of Ta. The value of that constant falls somewhat as Ta is increased; in the $\eta = 0{\cdot}8756$ case it falls from about $\frac{1}{2}$ to about $\frac{1}{3}$. In the $\mu = -0{\cdot}6$ case $\omega/m\Omega_1$ is only constant at Ta just above Ta_{w}. In the case $Ta = 2{\cdot}25\, Ta_{\text{v}}$, $\omega/m\Omega_1$ is no longer constant; waves with small m move considerably faster than waves with higher m. We should bear in mind that the frequencies obtained in figure 7 (b) are based on linearizing the wavy components of the motion; nevertheless, comparison with experiment would be of interest.

6. Conclusion

Overall there does seem to be good agreement between experiment and theory for the counter-rotating case. Particularly satisfactory is the agreement between experiment and theory over the strong preference for $m = 2$ in the transition to wavy-vortex flow at $\eta = \frac{1}{2}$. The calculated values of Ta_{w} and the frequencies in this case also seem to be compatible with observation. The predictions for the onset of waviness in the narrow gap case seem in reasonable agreement with what is known experimentally, although this region does not appear to have been covered quite so comprehensively as $\eta = \frac{1}{2}$. The only disagreement appears to be with Snyder's observation of the transition between non-axisymmetric flow and Taylor-vortex flow at $\eta = 0{\cdot}5$. The value found here, $\mu = -0{\cdot}39$, seems sufficiently different from the observed $\mu = -0{\cdot}44$ to require some explanation. We note, however, that at all the other values of η there is reasonable agreement, and that the correct value of m ($= 1$) is found, so perhaps this discordant note should not be overemphasized.

On the theoretical side, the main surprise is the behaviour of the nonlinear Taylor-vortex solutions shown in figure 2. The non-uniqueness, although it occurs even in the $\mu = 0$ case, does not appear to be in conflict with the uniqueness results of Kirchgassner & Sorger (1969), as their proofs only demonstrate the existence of an unspecified range of Ta above Ta_{v} in which there is a unique axisymmetric solution; the bifurcation described here lies at Ta greater than this range. It is not entirely clear whether this non-uniqueness has any practical consequence. It is possible, however, that it is connected with the shortening of the axial wavelength observed by Snyder at $\eta = \frac{1}{2}$.

I am grateful to Dr D. R. Moore for the loan of a program used to plot figure 6. I also acknowledge the co-operation of the Newcastle University Computing service for the use of the IBM 370/168 on which the computations were performed.

REFERENCES

BENJAMIN, T. B. & MULLIN, T. 1981 Anomalous modes in the Taylor experiment. *Proc. R. Soc. Lond.* A **337**, 221–249.

BOOZ, O. 1980 Numerische Lösung der Navier–Stokes-Gleichangen für Taylor-Wirbelströmungen im weiten Spalt. Ph.D. thesis, Stuttgart University.

CHANDRASEKHAR, S. 1958 The stability of viscous flow between rotating cylinders. *Proc. R. Soc. Lond.* A **246**, 301–311.

CHANDRASEKHAR, S. 1961 *Hydrodynamic and Hydromagnetic stability*. Clarendon.

CLENSHAW, C. W. 1955 A note on the summation of Chebyshev series. *Math. Tables & Aids to Computation* **9**, 118–120.

COLES, D. 1965 Transition in circular Couette flow. *J. Fluid Mech.* **21**, 385–425.

DAVEY, A., DIPRIMA, R. C. & STUART, J. T. 1968 On the instability of Taylor vortices. *J. Fluid Mech.* **31**, 17–52.

DIPRIMA, R. C. & EAGLES, P. M. 1977 An empirical torque relation for supercritical flow between rotating cylinders. *Phys. Fluids* **20**, 171–175.

DIPRIMA, R. C. & GRANNICK, R. N. 1971 A nonlinear investigation of the stability of flow between counter-rotating cylinders. In *Proc. IUTAM Symp.* 1969, *Instability of Continuous Systems* (ed. H. Leipholz), pp. 51–60. Springer.

DONNELLY, R. J. & FULTZ, D. 1960 Experiments on the stability of viscous flow between rotating cylinders. II. Visual Observations. *Proc. R. Soc. Lond.* A **258**, 101–123.

DONNELLY, R. J. & SCHWARZ, K. W. 1965 Experiments on the stability of viscous flow between rotating cylinders. *Proc. R. Soc. Lond.* A **283**, 531–546.

HILDEBRAND, F. B. 1956 *Introduction to Numerical Analysis*. McGraw-Hill.

JONES, C. A. 1981 Nonlinear Taylor vortices and their stability. *J. Fluid Mech.* **102**, 253–265.

KIRCHGASSNER, K. & SORGER, P. 1969 Branching analysis for the Taylor problem. *Quart. J. Mech. Appl. Math.* **22**, 183–209.

KRUEGER, E. R., GROSS, A. & DIPRIMA, R. C. 1966 On the relative importance of Taylor-vortex and non-axisymmetric modes in flow between rotating cylinders. *J. Fluid Mech.* **24**, 521–538.

MOORE, D. R. & WEISS, N. O. 1973 Nonlinear penetrative convection. *J. Fluid Mech.* **61**, 553–581.

MUSMAN, S. 1968 Penetrative convection. *J. Fluid Mech.* **31**, 343-360.

NAKAYA, C. 1975 The second stability boundary for circular Couette flow. *J. Phys. Soc. Japan* **38**, 576–585.

NISSAN, A. H., NARDACCI, J. L. & HO, C. Y. 1963 The onset of different modes of instability for flow between rotating cylinders. *A.I.Ch.E. J.* **9**, 620–624.

SNYDER, H. A. 1968 Stability of rotating Couette flow. I. Asymmetric waveforms. *Phys. Fluids* **11**, 728–734.

SNYDER, H. A. 1969*a* Wavenumber selection at finite amplitude in rotating Couette flow. *J. Fluid Mech.* **35**, 273–299.

SNYDER, H. A. 1969*b* Change in waveform and mean flow associated with wavelength variations in rotating Couette flow. *J. Fluid Mech.* **35**, 337–353.

VERONIS, G. 1963 Penetrative convection. *Astrophys. J.* **137**, 641–663.